Supporting Information

Characterizations

The crystal phase of synthesized powder was identified by X-ray diffraction (XRD, Bruker AXS D8-Focus, Germany) with Cu Kα radiation over the range of 2θ from 20 ^{o}C to 90 ^{o}C. The micromorphology of 2D *dr*-MoN powder was observed by means of a field emission scanning electron microscope (FESEM, Hitch SU8010, Japan) and a high-resolution transmission electron microscopy (HRTEM, FEI Tecnai G2) equipped with an energy-dispersive X-ray Spectroscope (EDS, EDAX Apollo XP, USA). The X-ray photoelectron spectrum (XPS, Escalab 250XI, ThermoFisher, USA) and atomic force microscopy (AFM, SPM9700, Shimadzu) were employed to further explore the chemical composition, structure and morphology of the samples. For the AFM measurements, the samples dissolved in the ethanol solution were dropped on flat mica plates and dried at room temperature. The specific surface area was determined by the Brunauer-Emmett-Teller (BET) method on the basis of the N_2 adsorption isotherm, and the mesopore distribution was analyzed by Barrett-Joyner-Halenda (BJH) method based on the data of the desorption branch using a TriStar II 3020 (Micromeritics Instrument Corporation, USA). The Raman spectra of as-obtained *dr*-MoN were acquired using a Renishaw System RM-1000 spectrometer.

Electrochemical measurements

All the electrochemical measurement, including cyclic voltammetry (CV), linear sweep voltammetry (LSV) and electrochemical impedance spectroscopy (EIS) tests were performed on Gamry (Interface 1000E, USA) electrochemical workstation with a conventional three-electrode system configuration. Typically, 4 mg 20% Pt/C catalyst or 4 mg respectively of as-produced 2D *dr*-MoN nano-sheets powder and N-doped carbon (NC) were dispersed in 700 mL deionized water, 300 mL ethanol and 11 μL Nafion solution by ultrasonic treatment for 1 h to form homogeneous suspension. NC was obtained by dispersing 600 mg of Vulcan XC-72 carbon in 100 mL sulfuric acid-nitric acid solution with a volume ratio of 3:1 via oil bath heating at 80 ^{o}C for 12 h, followed by filtration and an ammoniation process at 800 ^{o}C under NH_3 (5 vol% in argon) atmosphere for 8 h. Afterwards, 5 μL of the resultant ink (containing 20 μg of catalyst) was casted on GCE of 3 mm diameter and then air-dried, i.e. catalyst loading was 0.285 mg/cm^2. LSV at a scan rate of 2 mV/s was conducted under N_2-saturated 0.5 M H_2SO_4, 0.1M KOH and 1 M KOH solution using a graphite rod as the counter electrode, GCE with different catalysts as the working

electrode, SCE and Hg/HgO electrode as the reference electrode in acid and alkaline solutions, respectively. CV was carried out between 0.16 and 0.26 V at various sweep rates ranging from 20 to 200 mV/s to investigate the electrochemical double-layer capacitances, and between -0.3 and 0.2 V at 50 mV/s to study the cycling stability. EIS was performed over the frequency range from 1 MHz to 0.1 Hz with an applied perturbation voltage value of 10 mV as the excitation AC amplitude and DC voltage biased at a cathodic overpotential at 10 mA/cm^2 (η_{10}). For the amperometric (I-t) stability study, the working electrode was biased at η=150 mV under both acid and alkaline conditions for 20 h. All of the potentials were referenced to reversible hydrogen electrode (RHE).

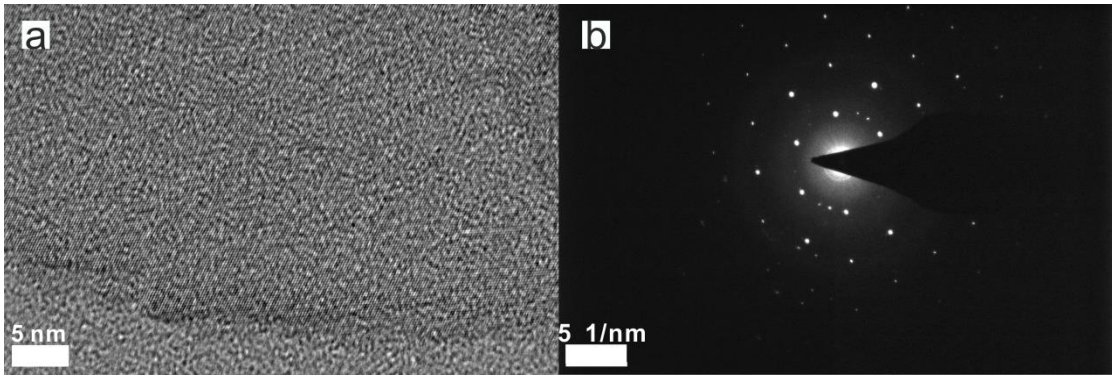

Figure S1. (a) The HR-TEM image and (b) the selected area electron diffraction (SAED) pattern of the *dr*-MoN-3 catalyst.

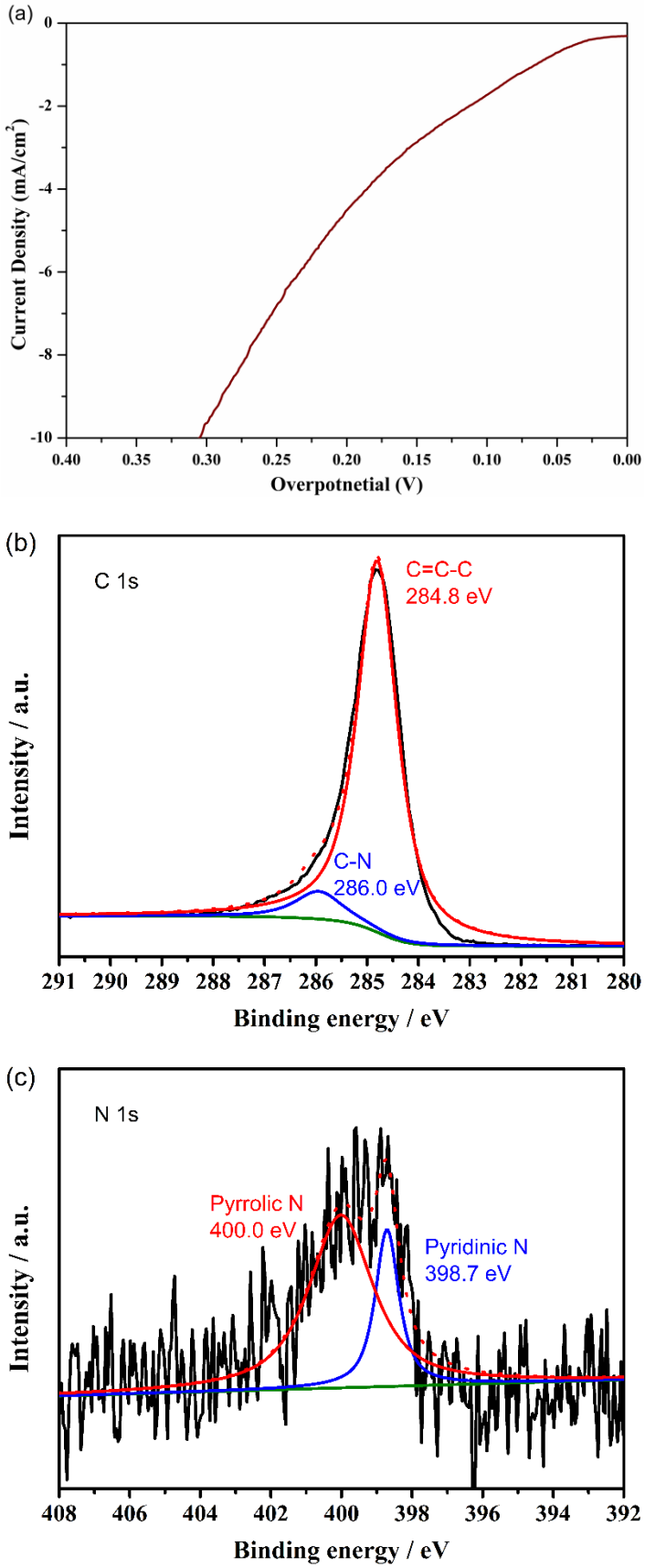

Figure S2. (a) LSV curve of HER on the bare N doped C carbon support in 0.5 M H_2SO_4 solution, the high-resolution XPS spectrum of (b) C 1s and (c) N 1s of N doped C.

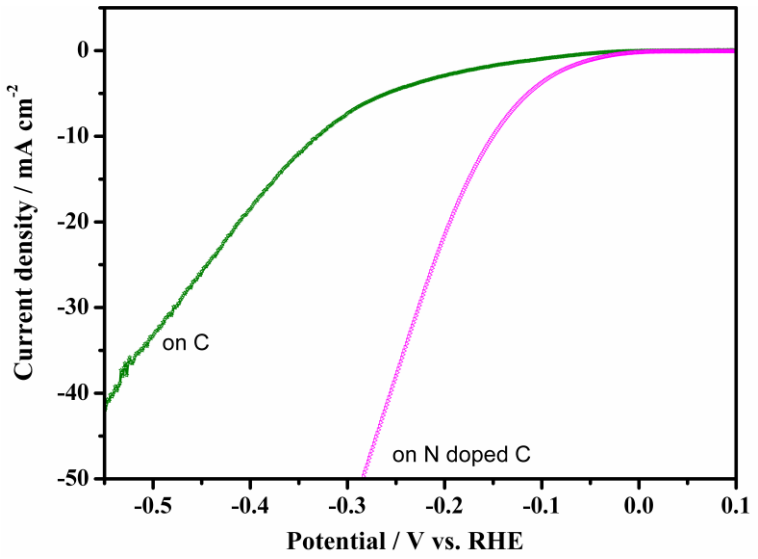

Figure S3. LSV curve of HER on the *dr*-MoN-1 catalysts doped on N doped C support and on the original carbon support in 0.5 M H_2SO_4 solution.

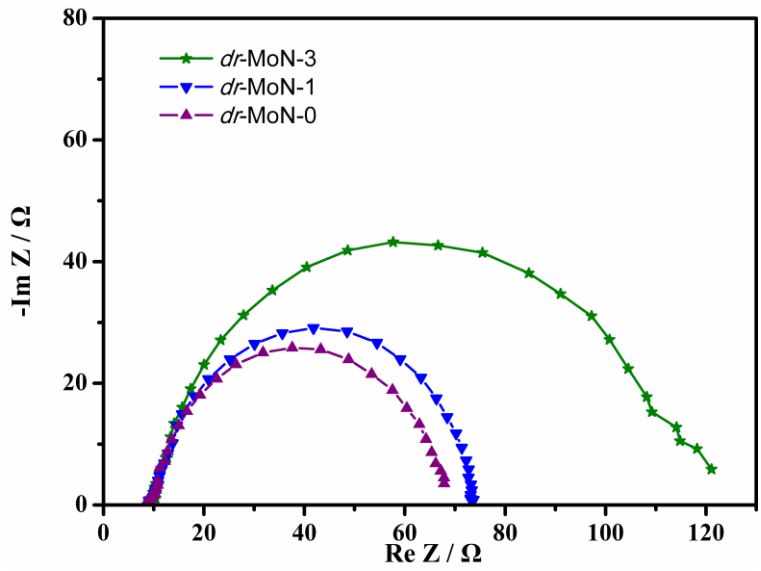

Figure S4. EIS spectra of the *dr*-MoN catalysts in 0.5 M H_2SO_4 solution at the potential of η_{10}.

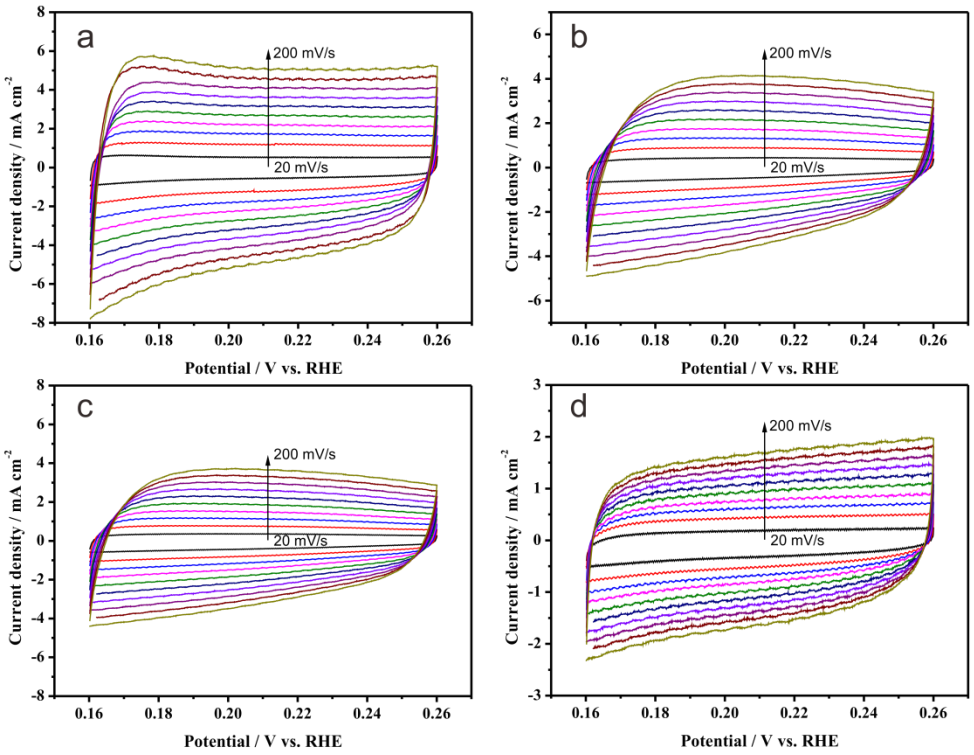

Figure S5. CV curves in 0.5 M H_2SO_4 solution obtained at various sweeping rates on the (a) the Pt/C, the *dr*-MoN-0, (c) the *dr*-MoN-1 and the *dr*-MoN-3 catalysts.

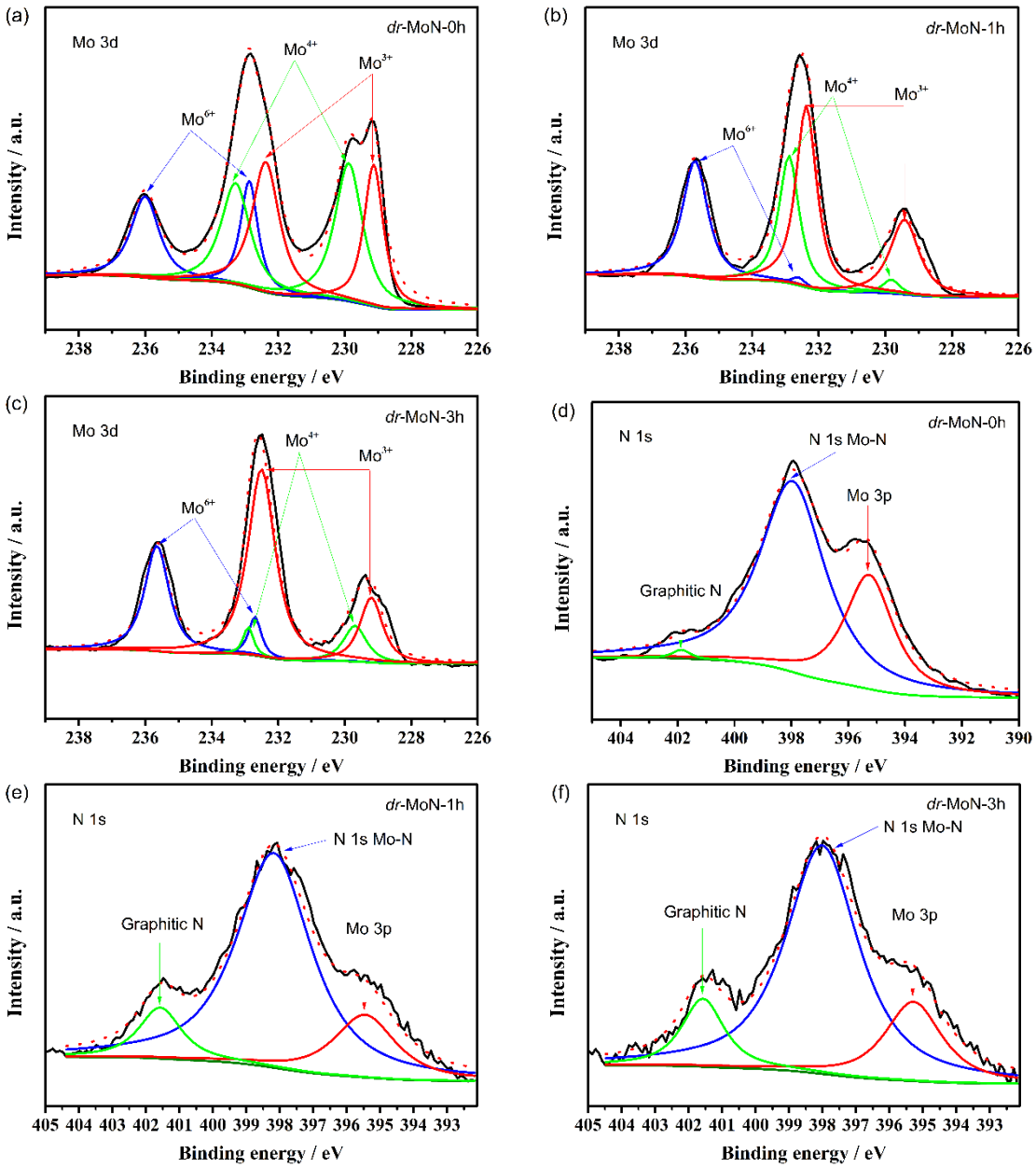

Figure S6. (a-c) High-resolution XPS patterns of Mo 3p and (d-f) N 1s of *dr*-MoN-0, *dr*-MoN-1 and *dr*-MoN-3.

From the normalized area of Mo^{3+} and N species (Mo-N), the chemical stoichiometric ratio of Mo^{3+} to N were determined to be 0.82, 1.01 and 1.29 for *dr*-MoN-0, *dr*-MoN-1 and *dr*-MoN-3, respectively. It should be noted that the high molar ratio of Mo^{3+} in the fully ammoniated *dr*-MoN-3 may arise from the unique sandwich structure of hexagonal MoN nano-sheets with one layer of N atoms sandwiched between two layers of Mo atoms exposed on the surface [Ref. S1]. Therefore, the Mo species are more sensitive in term of signal acquisition when XPS was performed to detect the surface chemical composition of MoN nano-sheets. However, the signal acquisition priority of superficial Mo atoms is gradually deprived with the increased Mo absence induced more exposure of active edge N sites in defect-abundant *dr*-MoN-1 and *dr*-MoN-0.

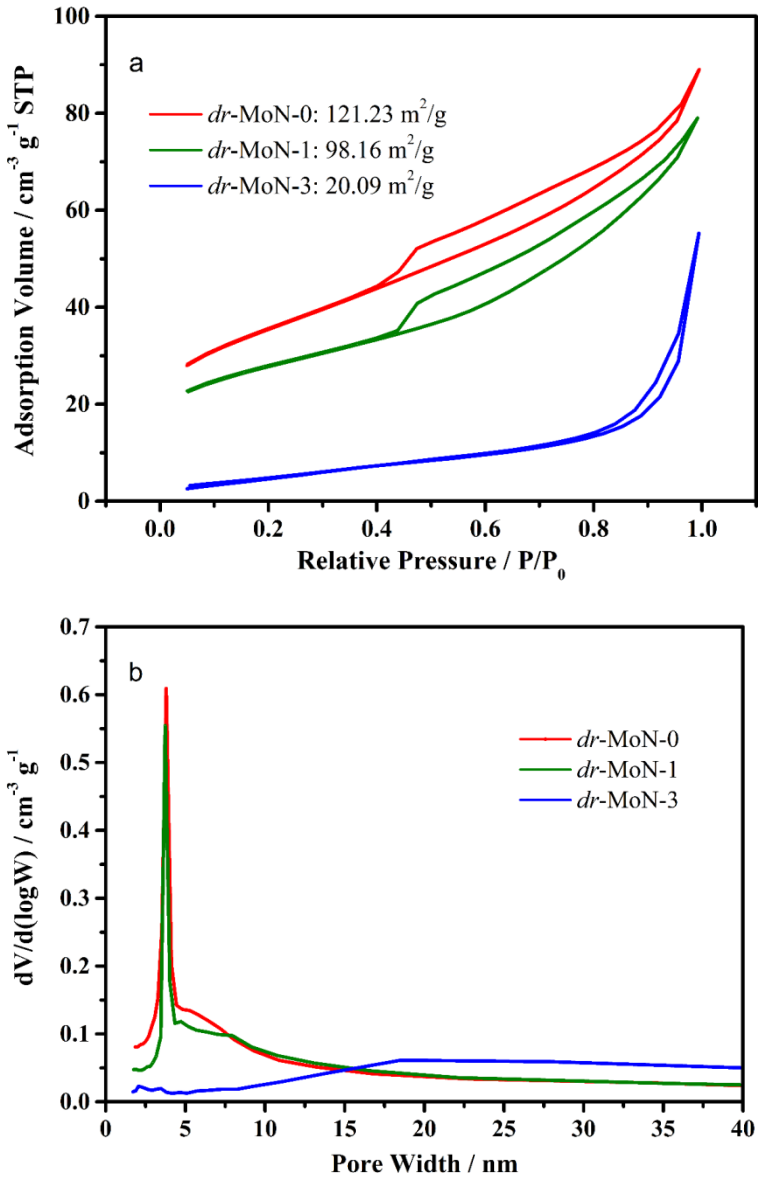

Figure S7. (a) The N_2 sorption isotherms and (b) the corresponding pore diameter distributions of *dr*-MoN-0, *dr*-MoN-1 and *dr*-MoN-3.

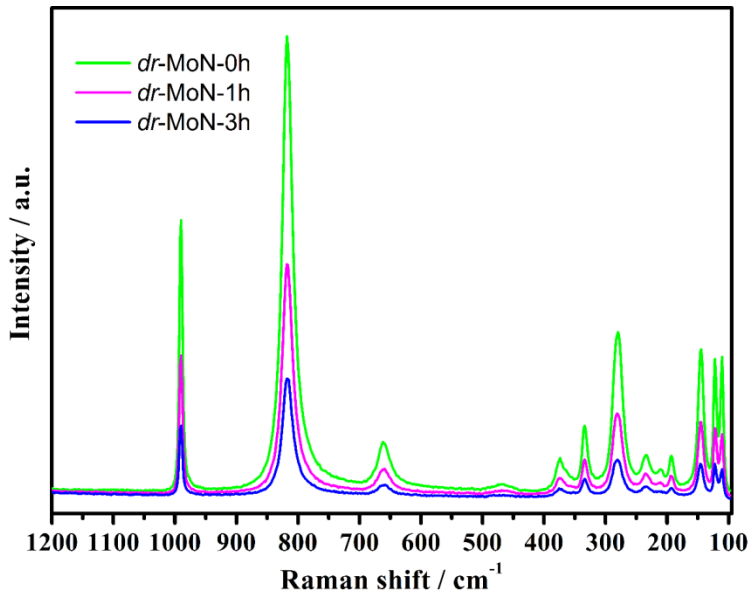

Figure S8. Raman spectra of *dr*-MoN-0, *dr*-MoN-1 and *dr*-MoN-3.

References

S1. J. Xie, S. Li, X. Zhang, J. Zhang, R. Wang, H. Zhang, B. Pan and Y. Xie, *Chemical Science*, 2014, **5**, 4615-4620.